Sensor Input Learning for Time-of-Flight Scan Laser

Mihaiela Iliescu*, Victor Vlădăreanu*[1], Mihai Şerbănescu, Marian Lazar*****

*Institute of Solid Mechanics, Romanian Academy,
Constantin Mille, 15, Bucharest, Romania,
** Centre of Advanced Laser Technologies (CETAL), National Institute for Laser, Plasma and Radiation Physics (INFLPR)
Atomistilor 409, Magurele, 077125 Romania
UPB Faculty of Electronics, Telecomunications and Information Technology, Splaiul Independenţei 313, 060042, Romania
*** SME OPTOELECTRONICA-2001,
Atomistilor 409, Magurele, 077125 Romania
1 Corresponding author*

Abstract: The paper presents the most important stages of product development for a new 2D TOF laser range sensor to be implemented in an autonomous platform. Some essential Scan-Laser characteristics are: measure in real-time, approximately, medium distances, works in high frequency, does not weigh much and is available at affordable prices. It has good power consumption and covers large scanning area with resolution lower than 1cm, all these makes if fit for various applications. Measurements of the distances to environmental objects is based on the principle Time-of-Flight (TOF). It consists in determining the distances by time span of transmitted and, consequently, received light waves. Mitigation of noise and disturbances effects is done by further processing collected data in learned neural networks model and statistical inference. Important characteristics of laser sensor prototype, its working principle for distance measurements, as well as some application and experimental results do really point out the potential and benefits of this prototype.

Keywords: laser beam, time of flight principle, spinning mirror, scan, sensor, neural networks, regression,.

1. INTRODUCTION

Nowadays, there are intelligent autonomous systems that rely on sensors for real time high performance 2D scanning of distances. Examples are evidenced by autonomous robots, systems for avoiding collision – on automotive market and self-guiding vehicles. The range of sensors available on the market for these type of application are expensive, relatively high weight and power consumption inefficiently for so many consumers.

Examples of sensors mentioned above are: LMS4xx - measurement of distances and contours with high precision; NAV3xx – for accurate laser navigation, made by SICK Sensor Intelligence (https://www.sick.com, 2017) or, ibeo LIDAR (Light Detection and Ranging) sensor - ensures good angular resolution, wide view field invaluable for precise and reliable mid-range detection (https://www.ibeo-as.com, 2017).

The paper evidences most important stages in development of 2D TOF laser sensor. Its design, concept development and manufacture of prototype were possible by collaboration of specialists from innovative SME, Centre of Advanced Laser Technologies and Institute of Solid Mechanics. Similar to most successful products, this Scan-Laser represents the result of joint effort from scientific research and industrial engineering, as, in fact, been pointed out by specialists and decision makers (McKelvey, OlofZaring, et al., 2015; Kalpana et al., 2015).

The new Scan-Laser product is an obstacle detection sensor featuring a compact, lightweight, power-efficient and low cost model, designed for implementation on an autonomous platform (Vlădăreanu, Dumitrache, et al., 2015).

For the market offer of TOF scanners there are no available data either on structure, design or, detection method. This paper evidences the innovation in design and manufacture by aspects mentioned next:

- Presents, for the first time, the methodology of TOF scanner design;
- New perspective for the setup of optical path (laser emitter and receiver) by its optimization and maximization;
- New perspective for determination of the distance to the target, by overlapping separate detection thresholds;
- New perspective applying neural intelligence in detection;
- New perspective of using mechanical rotational elements at high speed rotation with excellent dynamic equilibration.

Some technical characteristics of this laser scanner are: real time scanning distance till 50 m, , on black targets up to 5%; linear resolution of approximately 10 mm; 180º scanning angle field with angular resolution about 0.72º; scan frequency of 50Hz, that involves 12.500 scanning points per second; power consumption of 4W; relatively low production cost, above 1.000 Euro.

The paper further presents the most important stages of product development, implemented for the new product, Scan-Laser. These are congruent with the strategy outlined by Ulrich K.T. and Eppinger St. D. (2000), which consists in :

- Planning, that is presentation of development techniques, market objectives, etc;
- Concept development meaning identification of target market requirements;
- System design as the stage when product arrchitecture is defined and the subsytems and componets are settled;
- Detailed design when complete specifications of componments are defined and a elements to be supplied are identified;
- Testing and perfecting; that is manufacturing of the prototype, „zero series”,;
- Production - the „zero sery” and further, when any necessary adjustments done, the series, or mass production.

The remainder of the paper is divided as follows: Chapter 2 discusses the development of the scanner concept, focusing on the mathematical underpinnings and the chosen parameters. Chapter 3 presents the actual resulting design and prototype and Chapter 4 shows the input learning problem for the raw data coming from the sensor. Chapter 5 discusses the appropriate results and analysis, while Chapter 6 outlines the main talking points of the paper and attempts to draw a conclusion for future work.

2. CONCEPT DEVELOPMENT

This stage of new product development is based on the identification of target market requirements and the evaluation of alternative product concepts (Vargas et al., 2016).

Based on this, the laser sensor parameters that need to be extended, when compared to the characteristics of existing similar sensors should be mentioned as: scanning distance; wave frequency; measurements resolution, both angular and linear; reliability. .

This 2D laser sensor would be also designed to be integrated into the ERSEC measuring system - used on-board a vehicle able to output the position on the road map and of obstacles around it. Measurement data is obtained from an instrument set installed on board, including vehicle dynamic sensors (tachometer and gyro) and environmental sensors / scan lasers (http://www.ersecproject.eu/).

Based on these mentioned above, laser sensor parameters values were chosen as seen in Table 1. For competitive low price product, mass-produced components need to be used, are: regular laser diode, photoreceptor, low cost optics and common electronic components.

Table 1. Constraints of parameters values.

Characteristics	Constraint	Value
Distance to scan	the least	50 m
Frequency of scan wave	the least	50 Hz
	measure in real time	
Angular measure resolution	the most	1°
Distance measure resolution	the most	1 cm

The Scan-Laser product design parameters are detailed in (Şerbănescu, M., Iliescu M., et. al, 2014), but a review of the most important parameters considered for the design is given below.

The minimum modulation frequency for Time of Flight principle:

$$F_{\min} = \frac{100}{2.4165} = 41 \quad \text{[MHz]} \tag{1}$$

In fact, this frequency is not convenient for low cost systems, that is why it is only fit for use with Time-of-Flight (TOF) solution (Kostamovaara, Kurtti, et al., 2012).

Based on the telemetric low, equation for determining real laser power is : (Shapiro, Capron, et al., 1981):

$$\Pr = Pe \cdot \left(\frac{Ar \cdot Te \cdot Tr \cdot Kr}{4\pi \cdot d^2} \right) \cdot \exp(-2\tau d) \tag{2}$$

Significance of variables notation is evidenced in Table 2.

Table 2. Variables notation.

Pr	received power	Pe	receiving area
Ar	optical reception efficiency	Tr	emission power
Te	optical emission efficiency	Kr	target reflection coefficient
τ	atmospheric attenuation coefficient	d	distance to target

There are the limit conditions :

■ Pr-min = Pe / 561478 when scan distance is 50 m and there is regular black target (*Kr = 0.1*);

■ Pr-max = Pe / 2175 when scan distance is 0,3 m and there is regular white target (*Kr = 0.9*).

Real power emission should be of 40W so, it could be used OSRAM SPL-90_3 laser diode and OSRAM SFH 203PFA a reception photodiode (www.osram-os.com, 2014).

Envisaging optic geometry, there should be applied emission and reception that are collinear or quasi-collinear (parallel). In fact, the innovative affordable and simple solution consists in a spinning mirror enabling both collinear emission and reception. This desired co-linearity would be obtained by 50% beam splitter or by integrating emission into the optic receiver.

The scanner gain, defined for both cases are:

$$C = \frac{4 \cdot \Pr}{Pe \cdot K \cdot \pi} \tag{3}$$

If diameter value is *Dr=50mm*, for receiving optics, than it results the graph of gain variation versus laser emission diameter *De* – see Fig. 1.

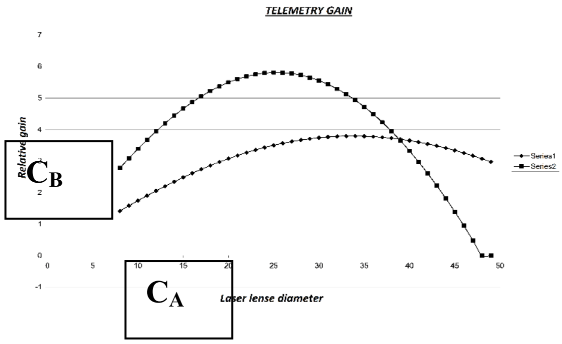

The gains $\mathbf{C_A}$ and $\mathbf{C_B}$ represent only mathematical system defined variables and do not have any physical equivalent;

Fig. 1. Variation of C_A and C_B, function of *De*.

Due to the aspects mentioned above, one can conclude that optimal choice is that of *emission integration into receiver optics*, with *De = 25mm,* as emission lens.

Important characteristics of the selected solution are: 45º angle positioned of spinning mirror; 3.000 rpm speed; Time-of-Flight principle for distance measurements with concentric laser emission and receiver optics,

The Time of Flight technique is based on emission moment of known value (www.osram-os.com, 2014). That is why, for the sensor, it is of great importance to have laser with integrated photodiode or, to have external photodiode across laser beam.

The innovative proposed solution for the sensor envisages exception of either previous requirements and application of TOF technique by direct determination of the time gap between laser command and target received signal. Thus, it appears a "dead" time, depending on electronic devices (gates, laser driver) in addition to measured time. It is characterised by slow variation in time, depending on temperature and power supply values.

This "dead" time could be eliminated if measurement of this delay were done at each rotation (or periodically), by performing an internal self-shot. In fact, the real distance will be measured from the sensor (output laser window) and not from the emission point of laser radiation.

Technical data are: laser pulses at periods of (40 ÷ 50) ns, , with signal front of about 7 ns. Laser signal rise time (front of signal) does generates an error with upper limit of 1m – as presented in Fig.2.

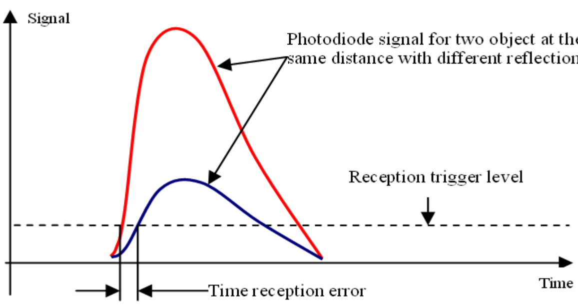

Fig. 2. Signals received.

Theoretically, this error could be eliminated, by determining the time gap of waves' peaks. In fact, received wave measurements do mean the sum of multiple reflection pulses. This is why, the technique would not appropriate.

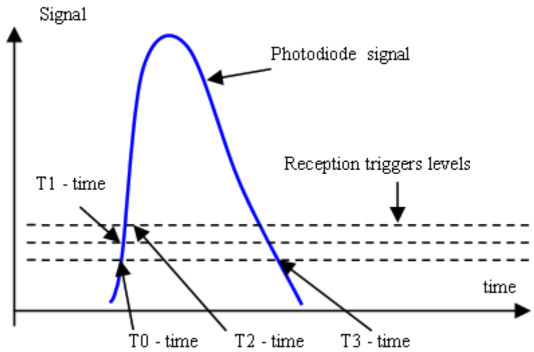

Fig. 3. Triggers signals received by photodiode.

As results of all the above, proposed solution is that of considering multiple trigger points for the signal front (rise time), as well as for the signal back (fall time) – shown in Fig. 3 So, 3 trigger points are applied at known levels for the purpose of determining time slope of signal, meaning T0, T1 T2 and T3. The result consist in determination of received signal's length.

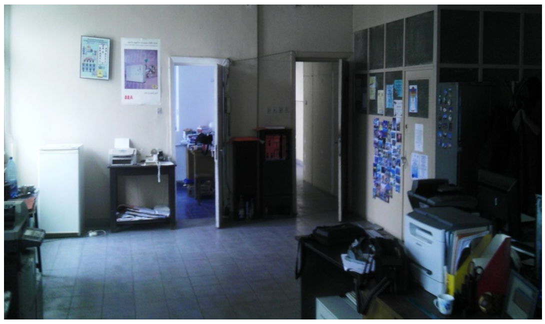

Fig. 4. The office room in experimental determination.

Scan points in an office room (presented in Fig.4) corresponding to moments: T0, T1, T2 and T3 are evidenced in Fig 5 and Fig. 6, There are determined estimated distance error in case of small signal back reflection - such as corners, postcards hang on walls etc.).

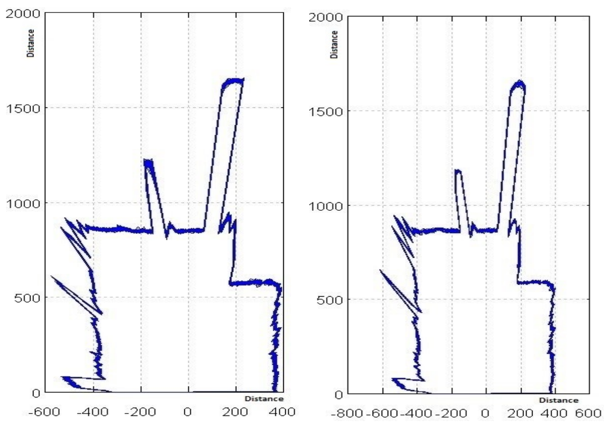

Fig. 5. Measurement of distances at T0 and T1.

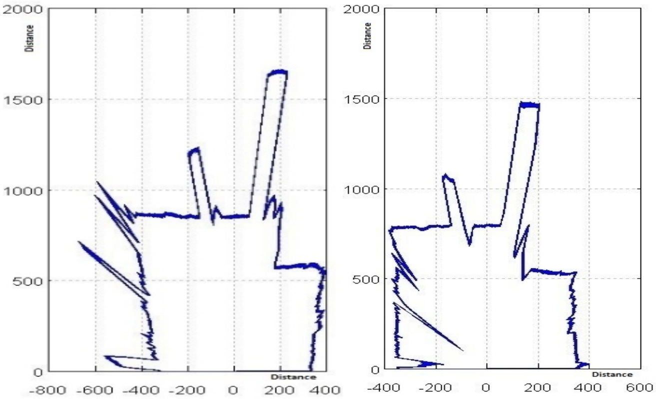

Fig. 6. Measurement of distances at T2 and T3.

All units are expressed in [cm], the graphs evidencing approximately 100 overlapped determinations. The thickness of graph plot line defines measurement noise (Șerbănescu, Iliescu, et. al., 2014).

It can be observed two open doors in the office room. In Fig.6 it is pointed out the small values for back-reflection (as, usually, it generates slope error) and for signal length when compared to length of the start laser signal (for closer objects). So, real room profile and distances could be identified by overlapping measurement results as in Fig.7.

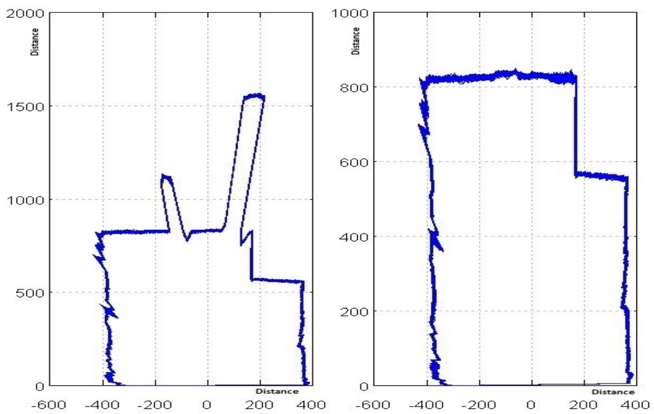

Fig.7. Determination of room profile – with open door (left graph) and closed door (right graph).

In Fig.4 one notices the postcards by the doors frame. On the left side, there are many postcards on the wall, and, consequently, the reflected signal has many variations of these reflections. This fits reality, as in the middle left of the plot graph (coordinates -400 and 400) it is suggested the postcard with one hanging corner – check Fig.7.

The right part of same figure evidences same office room, but with closed door (100 measurements overlapped).

These plotted data are obtained by approximately 100 determinations overlapped for data analyses and noise error estimations. The PC scanner software works in real time and the office room profile preview is generated by graph in Fig.8.

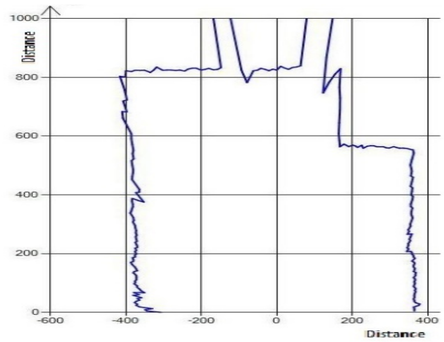

Fig. 8. Real time determination.

3. DESIGN AND PROTOTYPE

Fig. 9 presents the 3D model of the new product, Scan-Laser. Its main components are also named and positioned.

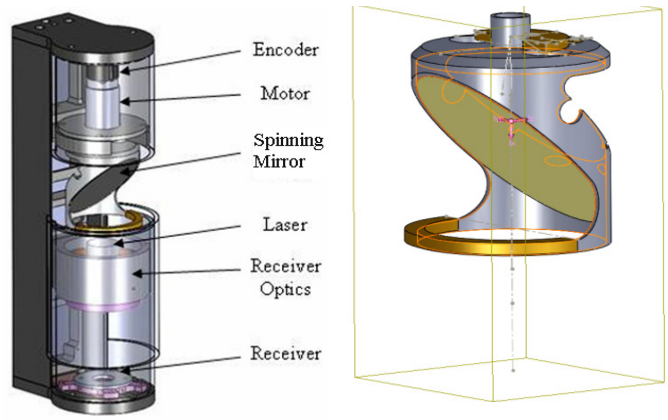

Fig. 9. Scan Laser Prototype.

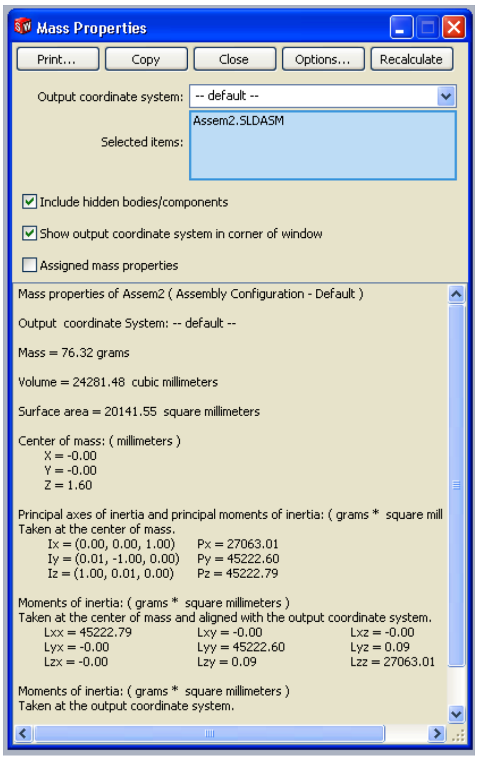

Fig. 10. Spinning mirror design.

The mechanical part of the scanner prototype was designed so as to ensure correct rotational axis for the spinning mirror subassembly, which should be perfectly aligned to the whole system axis. This is possible if there are same values for inertia moments on both OY and OZ axes, so as to be mechanical equilibrium of rotational system – see Fig. 10.

The materials of the spinning mirror subassembly components are as follows:
- Aluminium alloy – as low weight material for the main rotational component;
- Brass plates, made of AM63 – added as compensator weight for mechanical equilibrium when the spinning mirror rotates.
An image of the manufactured prototype subassembly is shown in Figure 11.

For accurate manufacturing of Scan-Laser prototype's main component, the spinning mirror, both turning and milling techniques were used (Iliescu M., 2011).

Turning on a CNC lathe ensured the cylindrical profiles of the spinning component, including the one being coupled to driving motor's spindle. Further, CNC milling, on 5 axes vertical centre, ensured the precise generation of this component complex inner surfaces.

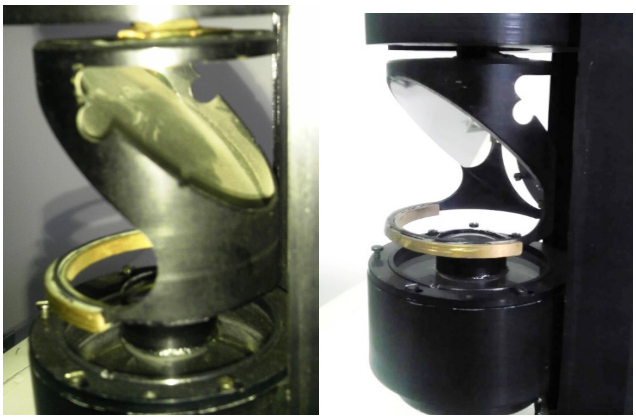

Fig. 11. Spinning mirror assembly manufactured prototype.

The brass plates, weight compensators, are accurately positioned by use of a video camera and then soldered to the required surfaces of main rotational component.

When all the system components are accurately fit together, dynamic calibration of the whole assembly is performed by rotating it at a 30 % higher value than the nominal rotational value in use.

Motor encoder is characterised by 500 increments and directly coupled index output

In measurements, laser pulse and start of chronometer were generated in correlation with encoder output. There was used MSC TDC-502 chronometer (www.msc-ge.com., 2014), with two channel 40 ps resolution counter.

The whole system is controlled from an ATMEL 8 bit microcontroller. For enabling external communications, there are used USB interface, serial interface with data communication speed 921.600 bauds or, CAN bus.

There is tilt adjustment for the laser assembly. Meanwhile, for centring focused back-reflection with photodiode there is used X-Y position adjustment for the receiver

The scheme of TOF Scan-Laser board is evidenced in Figure 12.

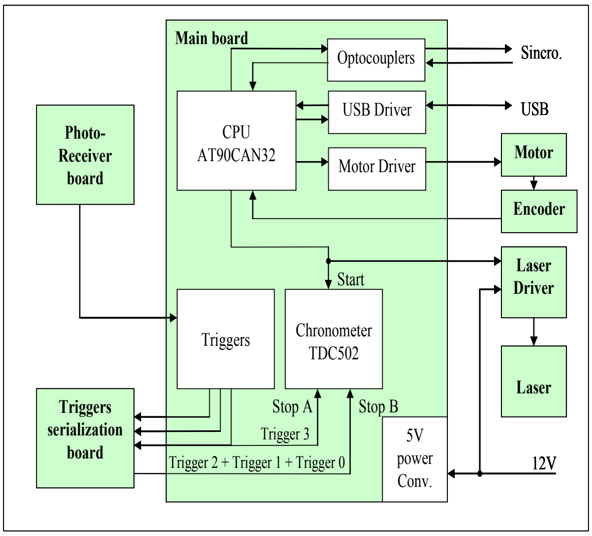

Fig. 12. Scheme of TOF Scan-Laser board.

The MSC TDC-502 is a versatile time measurement integrated circuit, capable of measuring time intervals between one common START impulse and multiple STOP impulses for two channels that work in parallel. The block diagram of the MSC TDC-502 is detailed in Figure 13.

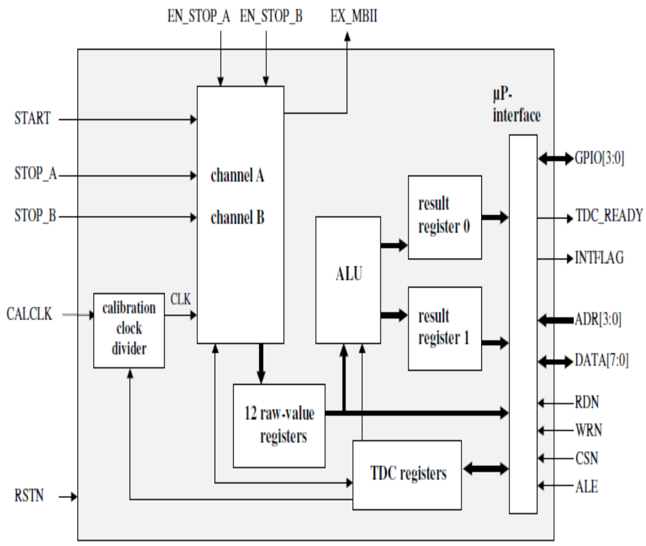

Fig. 13. Schematic board of chronometer.

The MSC TDC-502 can work in multiple time measurement configurations and for the specific scanner application the chosen working regime was with one START with two channels and four multiple STOPS each.

The minimum time distance between two consecutive stops on one channel is 25ns.The working time diagram is shown below (Figure 14):

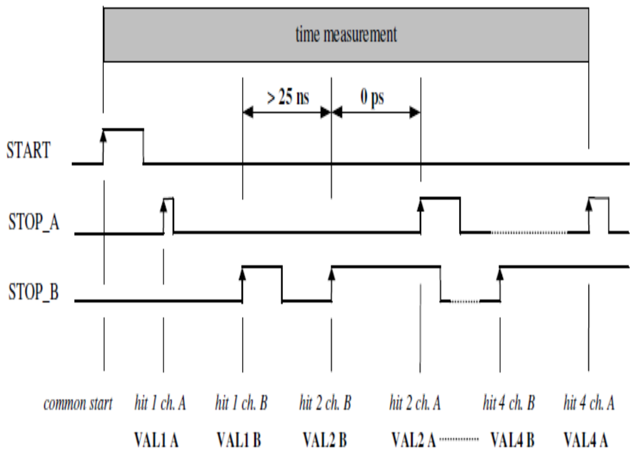

Fig. 14. Time measurement for TDC-502 in specific mode.

The three parallel triggers time with positive edge (T0,T1,T2) can be transformed into a serial signal with respect to T0,T1 and T2 times and a supplementary minimum 25ns between them – see Figure 15.

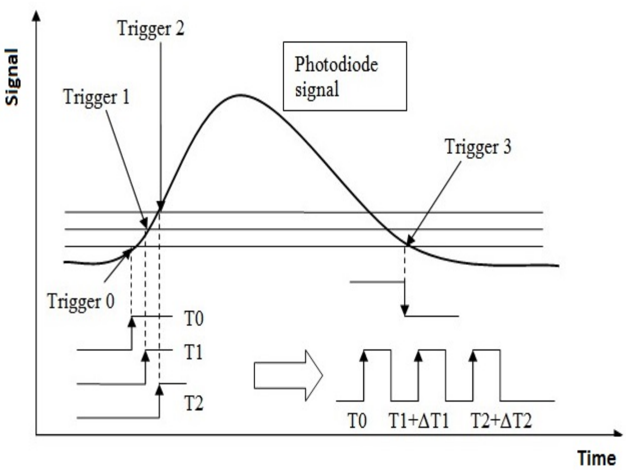

Fig.15. Serialization of triggers times.

The resulting serial trigger will have supplementary delays ΔT1 and ΔT2 but at each rotation that the system makes a laser self-shot internally (see Fig.2), these time delays are measured and are subtracted from the measurements of intervals T0, T1 and T3.

The only limitations for ΔT1 and ΔT2 are that they must be larger than 25ns - from the TDC-502 constraint. In the channels within TDC-502 one is used for the positive edge of the serial signal for T0, T1 and T2 and one for the negative edge for the T3 trigger signal.

In Fig. 16 there is shown a real field determination, with various environment, like: buildings (on top, right), grass and bushes (on left) and trees (in the middle).

The meaning of “0” value (see graphs above) is that of ”zero” back-reflection from the field, consequently, no information.

The real performance of the new Scan-Laser product, measured and determined for the manufactured prototype, is shown in Table 3.

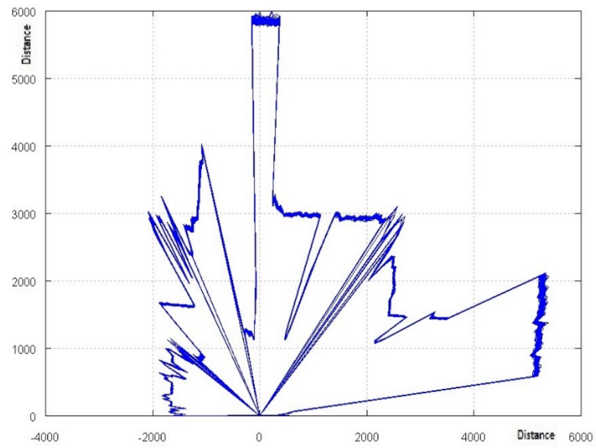

Fig. 16. Graph from real field determination .

Table 3. Performance parameters.

Distance to scan	60m
Frequency of scan wave	50Hz (3000rpm)
Angular scan angle	180º / 250 points
Distance measure resolution	1cm
Angular scan resolution	0.72º
Power supply	12V / 4W
Weight of prototype	850g
Dimensions of prototype	75 x 100 x 265mm
Estimated price	1.000 euros

One can notice that the estimated final price is significantly lower than the market offer of similar products.

4. DATA PROCESSING

The physical reality of the working environment makes processing the data received from the photodiode signal challenging. This is done using a number of trigger levels, as shown in Figure 3.

Under a certain threshold, signal measurement is indistinguishable from natural noise and is therefore unreliable. The first trigger is placed slightly above this level and detects a new signal. The next two triggers are placed on the rising slope and are useful for completing the model. The signals detected on each trigger are used as inputs, allowing estimates for the fourth.

The fourth trigger is on the falling slope, assuming an ideal signal with no interference. If this were reliably obtainable, it would allow for calculating the total time of the response signal, from which the distance to target is further inferred. While the theoretical approach seems to work, in practice several returning signals may interpolate into an unusable received signal. There is also the danger of higher amplitude noise being a factor in the sensor determination.

The problem statement can be summed up as follows. The measured distance was calculated at first as a function of the data on the first (T0) and last (T3) triggers, using a mathematical relation. In order to no longer rely on the fourth trigger measurement, due to the reasons discussed above, it is required to use the first three triggers (T0 – T2) to obtain reliable information on the fourth (T3).The chosen algorithm can then be hard-coded into the TOF scanner.

With the sensor in continuous scanning, the raw data from the first three triggers serves as inputs to a multivariate linear regression model, a multivariate polynomial regression model and a neural network model. For each point of the four triggers, the model was learned using the mean value out of 250 scans. These three approaches should, at the very least, provide a good understanding of how to further manipulate the input data to obtain the distance (Vlădăreanu, Şandru, et al., 2009). The numerical processing is done in Matlab/Octave. A sample of the raw data collected is shown in Table 4.

Table 4. Raw data example.

Nr	Trigger t0	Trigger t1	Trigger t2	Trigger t3 (target)
1	308.48	312.64	308.68	344.43
2	336.37	335.99	325.58	347.03
3	344.72	340.99	324.28	347.40
4	417.08	407.49	411.75	250.40
5	476.92	464.05	487.08	260.33
6	484.44	471.76	494.48	256.58
7	491.41	477.98	501.93	250.25
8	500.23	487.69	512.15	240.31
9	506.72	491.63	519.25	240.58
10	517.14	500.36	529.29	237.23
11	529.38	510.73	544.17	218.09
12	531.77	514.67	548.06	218.48
13	537.84	520.23	557.98	208.79
14	482.13	471.54	493.81	266.04
15	408.10	398.98	398.96	361.93
16	363.97	357.78	339.66	360.29
17	375.19	364.52	343.41	355.01
18	386.73	373.27	349.79	353.45
19	395.25	378.81	354.25	360.70
20	401.53	383.47	358.68	360.64
…	…			
245	374.41	363.86	330.56	373.04
246	374.94	363.49	330.90	360.63
247	375.53	363.60	331.48	357.23
248	376.78	365.47	332.56	356.76
249	378.93	366.25	333.34	355.38
250	376.21	364.37	331.99	354.25

The first model is a multivariate linear regression. The optimisation problem is described as:

$$Y = \hat{\theta} \cdot X \tag{4}$$

$$X = [X_1 \quad X_2 \quad X_3] \tag{5}$$

with:

X is the input data of the three triggers (T0 – T2), contained inside a matrix with all 250 space points, plus an intercept term;

Y is the output data of the fourth trigger (T3), that the algorithm is trying to learn, represented a vector containing all space point values;

$\theta$is the matrix of parameters used to estimate Y from X.

The challenge is finding the bestΘ which minimizes the error between the actual Y and the estimate. This is obtained from:

$$\hat{Y} = \theta_{LR} \cdot X \tag{6a}$$

or, in extended form:

$$\begin{bmatrix} \hat{y}_1 \\ \hat{y}_2 \\ \hat{y}_3 \\ \vdots \\ \hat{y}_n \end{bmatrix} = \begin{bmatrix} \theta_{11} & \cdots & \theta_{1(m+1)} \\ \vdots & \ddots & \vdots \\ \theta_{n1} & \cdots & \theta_{n(m+1)} \end{bmatrix} \cdot \begin{bmatrix} x_1 \\ x_2 \\ \vdots \\ x_m \\ \text{int} \end{bmatrix} \tag{6b}$$

As can be seen, there will be *m* features and an intercept term, which helps prevent over-fitting.

The total sum of all errors, across all values, is defined as the cost function J. (Vlădăreanu, V., 2014)

$$J = \sum_{i=1}^{250} \left| \hat{y}_1 - y_i \right| \tag{7}$$

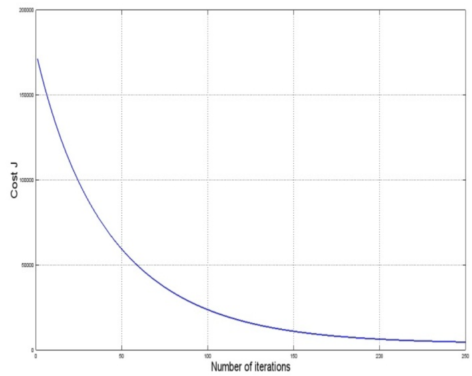

Fig. 17. Linear Regression Cost Function.

The first step in a multiple variable regression model is to normalize the features and then run a batch gradient descent algorithm on the data, where each iteration minimizes the cost function by simultaneously updating all Θ parameters.

Figure 17 shows a plot of the cost function J against the number of iterations (or epochs) of the gradient descent algorithm. As can be plainly seen the cost function decreases constantly to a convergent value.

Gradient descent is an optimization algorithm where the potential solution is improved each iteration by moving along the feature gradient in the variable space. While it requires that the target function be differentiable and it is somewhat susceptible to local minima, gradient descent provides a stable and computationally inexpensive algorithm for function optimization.

There are a number of variants for gradient descent; the algorithm of choice here is batch gradient descent with a unity learning rate.

The same result can be achieved by using the closed-form solution to linear regression, called the normal equations of the problem. In vector form, this is:

$$\theta = \left(X^T \cdot X\right)^{-1} \cdot X^T \cdot \bar{y} \tag{8}$$

which does not require any initial feature scaling.

5. RESULTS AND ANALYSIS

Figure 18 shows the actual Y parameter against the estimation obtained from linear multivariate regression.

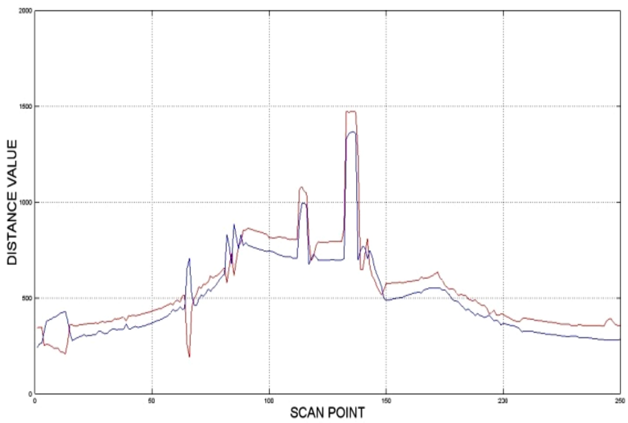

Fig. 18. Real (red) and predicted (blue) values for single-order features.

To obtain a better fit, a linear regression model using higher-order features is investigated. The process is in essence the same with the important difference that we are trying to fit the data using a polynomial expression which includes all combinations of variables up to the sixth power.

The new hypothesis is described as follows:

$$Y = \hat{\theta} \cdot X \tag{9}$$

$$X = [X_1 \;\; X_2 \;\; X_1X_2 \;\; X_1^2 \;\; \dots \;\; X_2^6] \tag{10}$$

As shown in Figure 19, the predicted values are closer to the known values measured empirically for Y.

Both versions of the linear regression model include regularization factors to prevent over-fitting. The regularization component is included in the cost function and provides a penalty for the data being fitted too closely using the polynomial variables.

The third investigated model is an artificial neural network. Atypical topography for such networks is shown in Figure 20 (Templeton, 2015).

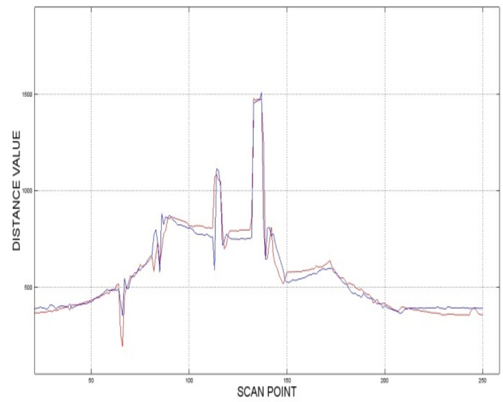

Fig. 19. Real (red) and predicted (blue) values for multi-order features.

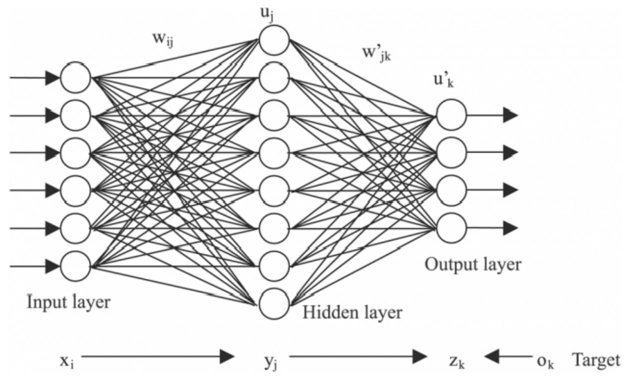

Fig. 20. Artificial Neural Network with one hidden layer.

As is usually the case with training neural networks, approximately 70% of the available raw data is used for training, 20% for cross-validation after the initial training scenario, and 10% for testing. Figure 21 shows the best data fit obtained fro man artificial neural network. As can be seen in this and in Figure 22, it provides the closest match of any of the three methods.

After training, each of the models can be used to generate new estimates given similar inputs.

For this particular run of the neural network, the accuracy quotas are shown in Table 5.

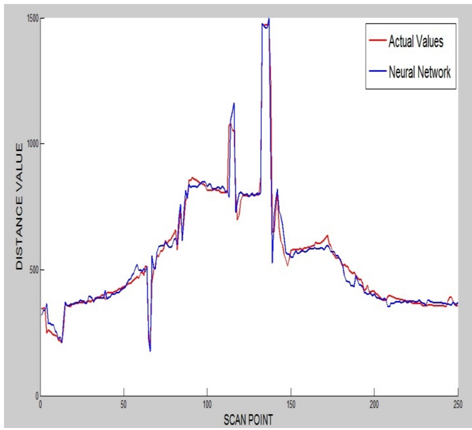

Fig. 21. Comparison of real (red) and predicted values (blue) for a neural network.

Table 5. Neural Network Performance.

Train Performance	1244.7
Validation Performance	904.0471
Test Performance	1463.2

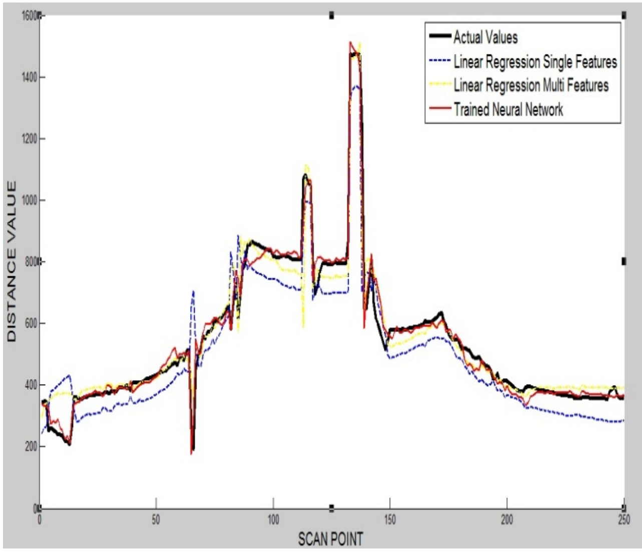

Fig. 22. Comparison of real (black) and predicted values from all models.

The results of the parameter estimation for all models using multivariate linear and polynomial regression and a trained artificial neural network are shown in Figure 22.

The final results for the accuracy of each method is shown in Table 6, which comprises the total cost for each method, as the sum of all absolute errors when using the particular model.

As a result, the selected implementation to be hard-coded into the TOF Laser prototype is the artificial neural network with the weights obtained through running multiple scenarios, as described in Section 4. A logging system is also put in place, so that the neural network weights may be retrained after a period of operation. This will lead to better results being obtained from the raw data, as well as being able to involve the prototype in actual situations (both static and dynamic) as part of a complex autonomous mechatronic platform – see reference (Vlădăreanu, Tonț, et al., 2010), which will allow for further testing with more practical results.

Table 6. Final estimation costs.

Method	Cost
Regression: Single-order features	19413.6
Regression: Multi-order features	9198.6
Neural Network	5651.2

6. CONCLUSION

This article points out main steps in the design and development of a two-dimensional TOF laser sensor fit for various autonomous platforms, among many other possible applications (Repta, Moisescu, et al., 2017).

The key component of the new product, 2D TOF Scan laser is the spinning mirror. The prototype was designed and, further manufactured, so as to ensure a perfect rotational axis for the spinning mirror subassembly, accurately aligned to the whole system axis.

This scan laser prototype is characterised by: real-time measurements; high frequency waves; medium-distance scanning; lightweight construction; affordable low price, low power consumption required. It provides real wide scan angle with high resolution (1cm at more than 50 m).

The raw results are processed from a trained artificial neural network obtained after thorough testing and comparison with other potential solutions. This allows an efficient software solution aimed at reducing measurement errors, which can be implemented on-board the actual sensor controller, as the neural net weights do not need to be retrained, unless significant hardware changes are made.

Further research will be developed toward optimization of this laser sensor focused on: decreasing scan errors; smaller dimensions and more reliable structure; finding opportunities for its market transfer, as well as interfacing with more complex autonomous systems for which several tests have been already run.

The prototype is a first step towards building low cost, high quality equipment to be seamlessly integrated into meaningful applications, overcoming innate physical hardware deficiencies with the aid of artificial intelligence algorithms and methodology.

ACKNOWLEDGEMENT

“This work was accomplished through the research programs:

- Partnerships Program in priority fields - PN II, developed with the support of MEN-UEFISCDI, PN-II-PT-PCCA-2013-4, ID2009, VIPRO project no.009/2014, Romanian Academy

- FP7-PEOPLE-2012-IRSES RABOT project no. 318902-FP7 ERSEC project, Enhanced Road Safety by integrating Egnos-Galileo data with on-board Control system (http://www.ersecproject.eu/)”

REFERENCES

http://www.optoel.ro/, accessed on November, 2015

Hybrid Pulsed Laser Diode 70 W Peak Power SPL LL90_3. & Silicon PIN Photodiode SFH203PFA & Range Finding Using Pulse Lasers Application Note OSRAM, www.osram-os.com, accessed on October, 2014

IBEO ScanLaser Products, http://www.ibeo-as.com

Iliescu, M., “Customized Products Manufacturing”, Published by WSEAS Press, ISBN 978-960-474-303-2, 2011,

Kalpana, D., Thyagarajan, T., Thenral, R., Improved Identification and Control of 2-by-2 MIMO System using Relay Feedback, *Control Engineering and Applied Informatics Journal*, CEAI, Vol.17, No.4 pp. 23-32, 2015, ISSN 1454-8658.

Kostamovaara, J. ,Kurtti, S., Jansson, J.P. "A receiver – TDC chip set for accurate pulsed time-of-flight laser ranging", CDNLive! EMEA 2012, accessed at https://www.google.ro/webhp?sourceid=chrome-instant&ion=1&espv=2&ie=UTF-8#q=functionality+limist, on April, 20, 2015

McKelvey, M., OlofZaring, O., Ljungberg, D., Creating innovative opportunities through research collaboration: An evolutionary framework and empirical illustration in engineering, Technovation39-40(2015)26–36,

Repta, D., Moisescu, M. A., Sacala, I. S., Dumitrache, I., & Stanescu, A. M. (2017). Towards the development of semantically enabled flexible process monitoring systems. *International Journal of Computer Integrated Manufacturing*, *30*(1), 96-108.

Serbanescu, M., Iliescu, M., Lazar, M., Ciufudean, C., "Development of 2D, Ultra-Simple, Low-Cost, Optical Range TOF ScanLaser", Proceedings of the 5th International Conference on Circuits, Systems, Control, Signals (CSCS '14), pg. 91-96, ISSN: 1790-5117, ISBN: 978-960-474-374-2, Salerno, Italy, June, 2014.

Shapiro, J, Capron, B and Harney, R, Imaging And target detection with a heterodyne reception optical radar; Applied Optics, vol. 20 pp 3292 -3313, October 1981

SICK Products LMS5XX ScanLaser, https: //www.mysick.com, accessed on October, 2014

TDC 502 user manual, www.msc-ge.com., accessed on September, 2014

Templeton, G., Artificial neural networks are changing the world. What are they?, https://www.extremetech.com/ extreme/215170-artificial-neural-networks-are-changing-the-world-what-are-they

Ulrich, K. ., Eppinger, S.D. Product Design and Development, McGraw-Hill Companies, USA, 2000

Vlădăreanu, L., Sandru, O., Velea, L., Yu, H., The Actuators Control in Continuous Flux using the Wiener Filters, Proceedings of Romanian Academy, Series A, vol.: 10 Issue: 1 Pg.: 81-90, 2009, ISSN 1454-9069

Vlădăreanu, L., Tont, G., Ion, I., Munteanu, M., S., Mitroi, D., "Walking Robots Dynamic Control Systems on an Uneven Terrain", Advances in Electrical and Computer Engineering, e-ISSN 1844-7600, vol. 10, no. 2, pp. 146-153, 2010,

Vlădăreanu, V., Contributions to intelligent control of autonomous robots equipped with multi-sensors systems, Ph.D. Thesis (summary), http://www.scribd.com/doc/ 274267670/Contributions-to-intelligent-control-of-autonomous-robots-equipped-with-multi-sensors-systems, Politehnica University Bucharest, 2014

Vlădăreanu, V., Dumitrache, I., Vlădăreanu, L., Sacala, I. S., Tont, G., & Moisescu, M. A. (2015). Versatile intelligent portable robot control platform based on cyber physical systems principles. *Stud. Informat. Control*, *24*(4), 409-418.

Vargas, A., Day, S., Boza, A., Ortiz, A., Ludäscher, B., Sacala, I., S., Moisescu, M., A., Decision-Making System and Operational Risk Framework for Hierarchical Production Planning, *Control Engineering and Applied Informatics Journal*, CEAI, Vol.18, No.2 pp. 72-81, 2016, ISSN 1454-8658.